Medium-Term Planning of Active Distribution Systems Considering Voltage-Dependent Loads, Network Reconfiguration, and CO_2 Emissions

Mario A. Mejia[1], Leonardo H. Macedo[1*], Gregorio Muñoz-Delgado[2], Javier Contreras[2], and Antonio Padilha-Feltrin[1]

1- Department of Electrical Engineering, São Paulo State University, Avenida Brasil 56, Centro, Ilha Solteira, 15385-000, SP, Brazil
2- Escuela Técnica Superior de Ingeniería Industrial, Universidad de Castilla-La Mancha, 13071 Ciudad Real, Spain

Abstract

This work proposes a novel mixed-integer linear programming model to address the medium-term reinforcement planning for active distribution networks, taking into account multiple investment options and CO_2 emission limits. The investment plan jointly includes (i) the replacement of overloaded conductors, (ii) the installation of voltage control equipment such as voltage regulators and capacitor banks, and (iii) the installation of distributed energy resources, such as dispatchable and non-dispatchable renewable generators, and energy storage units. Uncertainties associated with the demand for electricity, energy prices at the substation, and non-dispatchable distributed generation are addressed through scenario-based stochastic optimization. In contrast to conventional planning methods, the proposed approach models the load as voltage-dependent in order to achieve substantial reductions in energy consumption. As another outstanding feature, network reconfiguration, which is an operational planning alternative that is normally addressed independently, is incorporated within the planning options. The objective function of the model is aimed at establishing an investment strategy with minimal total costs, but that satisfies the operational restrictions of the network and CO_2 emissions cap. A 69-node system was used to test the proposed model and, the results show that modeling the load as voltage-dependent and integrating network reconfiguration into the medium-term planning actions helps to achieve an effective network that, in addition to being environmentally friendly, has low total planning costs. Finally, the scalability of the proposed method was evaluated using a real 2313-node system.

Keywords: Active distribution networks, mixed-integer linear programming, network reconfiguration, renewable distributed generation, voltage-dependent loads.

Nomenclature

Sets:

Γ^B	Set of branches, with index ij
Γ^G	Set of dispatchable distributed generation types, with index ϱ
Γ^L	Set of conductor types, with index a
Γ^N	Set of nodes, with index i
Γ^S	Set of scenarios, with index s
Γ^{SS}	Set of substation nodes, with index i

Parameters:

$\Phi_i^Z, \Phi_i^I, \Phi_i^P$	Constant impedance/current/power components of the active load at node i
$\Upsilon_i^Z, \Upsilon_i^I, \Upsilon_i^P$	Constant impedance/current/power components of the reactive load at node i
$\overline{S}^{PV}, \overline{S}^{WT}$	Apparent power capacity of a photovoltaic/wind turbine unit
$\overline{S}_i^{SS}$	Apparent power capacity of the substation at node i
$\overline{S}_\varrho^G$	Apparent power capacity of the dispatchable distributed generation unit of type ϱ
$\overline{P}^{ES}$	Nominal active power capacity of an energy storage unit

*Principal corresponding author
E-mail addresses: mario.andres@unesp.br (Mario A. Mejia); leohfmp@ieee.org (Leonardo H. Macedo); Gregorio.Munoz@uclm.es (Gregorio Muñoz-Delgado); Javier.Contreras@uclm.es (Javier Contreras); antonio.padilha-feltrin@unesp.br (Antonio Padilha-Feltrin).

Ω_s	Indicates the block in which scenario s belongs for the exchange of energy among scenarios
$\overline{I}_a$	Current capacity of the conductor of type a
$\mathcal{L}_{ij}$	Length of branch ij
V^N	Nominal voltage of the system
$\tilde{V}_{i,s}$	Estimate of the voltage magnitude at node i, scenario s
Δ_s^T	Duration of scenario s
$\underline{V}$, $\overline{V}$	Lower/upper voltage limits
$\underline{PF}_\varrho^G$, $\overline{PF}_\varrho^G$	Capacitive/inductive power factor limits of the dispatchable distributed generation unit of type ϱ
$\underline{PF}^{PV}$, $\overline{PF}^{PV}$	Capacitive/inductive power factor limits of photovoltaic units
$\underline{PF}^{WT}$, $\overline{PF}^{WT}$	Capacitive/inductive power factor limits of wind turbine units
$\mathcal{C}_s^E$	Energy price for scenario s
$\mathcal{V}_{\dot{a},a}^L$	Cost to replace the conductor of type $\dot{a}$ by the conductor of type a per unit of length
$\mathcal{V}^{CB}$, $\mathcal{J}^{CB}$	Investment/installation costs of capacitor banks
$\mathcal{V}^{ES}$, $\mathcal{C}^{ES}$	Investment/operation costs of energy storage units
$\mathcal{V}^{PV}$, $\mathcal{C}^{PV}$	Investment/operation costs of photovoltaic units
$\mathcal{V}^{WT}$, $\mathcal{C}^{WT}$	Investment/operation costs of wind turbine units
$\mathcal{V}_a^{VR}$	Cost of the voltage regulator of type a
K^{VR}	Regulation of voltage regulators
$\mathcal{V}_\varrho^G$, $\mathcal{C}_\varrho^G$	Investment/operation costs of the dispatchable distributed generation unit of type ϱ
$\mathcal{B}^{CB}$	Capacitor bank module's susceptance
$P_{i,s}^D$, $Q_{i,s}^D$	Active/reactive power demands at node i, scenario s at nominal voltage
R_a, X_a, Z_a	Resistance/reactance/impedance of the conductor of type a per unit of length
$\mathcal{E}^{PV}$, $\mathcal{E}^{WT}$, $\mathcal{E}^{SS}$	Rates for CO_2 emissions of photovoltaic units/wind turbine units/substations
$\mathcal{E}_\varrho^G$	Rate for CO_2 emissions of the dispatchable distributed generation unit of type ϱ
$\mathcal{F}_s^{PV}$, $\mathcal{F}_s^{WT}$	Generation factor of photovoltaic/wind turbine units in scenario s
$\mathcal{X}^{ES^c}$, $\mathcal{X}^{ES^d}$	Efficiencies for charging/discharging the energy storage units
$\overline{\mathcal{N}}^{VR}$	Limit for the number of voltage regulators in the system
$\overline{N}_i^{CB}$, $\overline{\mathcal{N}}^{CB}$	Limits for the number of capacitor bank's modules installed at node i/capacitor banks in the system
$\overline{\mathcal{W}}_i^G$	Binary parameter that indicates whether node i is a candidate for the installation of a dispatchable distributed generation unit
$\overline{\mathcal{N}}^G$	Limit for the number of dispatchable distributed generation units installed in the system
$\overline{N}_i^{ES}$, $\overline{\mathcal{N}}^{ES}$	Limits for the number of energy storage units installed at node i/in the system
$\overline{N}_i^{PV}$, $\overline{\mathcal{N}}^{PV}$	Limits for the number of photovoltaic units installed at node i/in the system
$\overline{N}_i^{WT}$, $\overline{\mathcal{N}}^{WT}$	Limits for the number of wind turbine units installed at node i/in the system
Π	Annual rate of interest
$\overline{\Lambda}$	Annual limit for CO_2 emissions
Θ	Number of years in the planning horizon
LF_t	Load factor for year t
$\overline{\Delta}_{ij}^{\hat{S}}$	Length of a block of the total power flows linearizations for branch ij
$\mathcal{M}_{ij,\psi}^{\hat{S}}$	Slope of block ψ of the total power flows linearizations for branch ij
Ψ	Number of discretization blocks used in the piecewise linearizations

Continuous Variables:

IC, OC	Investment/operation costs
$p_{i,s}^{PV}$, $q_{i,s}^{PV}$	Active/reactive power injected by photovoltaic units at node i, scenario s
$p_{i,s}^{SS}$, $q_{i,s}^{SS}$	Active/reactive power injected by the substation at node i, scenario s
$p_{i,s}^{WT}$, $q_{i,s}^{WT}$	Active/reactive power injected by wind turbine units at node i, scenario s

$p^{G}_{i,\varrho,s}$, $q^{G}_{i,\varrho,s}$ Active/reactive power injected by the dispatchable distributed generation unit of type ϱ at node i, scenario s

$p_{ij,a,s}$, $q_{ij,a,s}$ Active/reactive power flows on the conductor of type a, on branch ij, scenario s

$\hat{p}_{ij,s}$, $\hat{q}_{ij,s}$ Total active/reactive power flows on branch ij, scenario s

$\omega^{V}_{ij,s}$ Variable used to represent the voltage difference across the voltage regulator on branch ij, scenario s

$\vartheta_{ij,s}$ Slack variable for the voltage drop equation on branch ij, scenario s

$\hat{p}^{+}_{ij,s}$, $\hat{p}^{-}_{ij,s}$ Nonnegative variables used for the active power flow linearization on branch ij, scenario s

$\hat{q}^{+}_{ij,s}$, $\hat{q}^{-}_{ij,s}$ Nonnegative variables used for the reactive power flow linearization on branch ij, scenario s

$\delta^{\hat{p}}_{ij,\psi,s}$, $\delta^{\hat{q}}_{ij,\psi,s}$ Contribution in the total active/reactive power flows of the linearization block ψ, on branch ij, scenario s

f_{ij} Fictitious flow on branch ij for ensuring the connectivity of the network

g_{i} Fictitious generation at node i for ensuring the connectivity of the network

$\imath^{SQ}_{ij,a,s}$ Squared value of the current through conductor of type a, on branch ij, scenario s

$\hat{\imath}^{SQ}_{ij,s}$ Total squared value of the current through branch ij, scenario s

$p^{ES^{c}}_{i,s}$, $p^{ES^{d}}_{i,s}$ Active power related to the charge/discharge of the energy storage units at node i, scenario s

$q^{SH}_{i,c,s}$ Reactive power injected by the capacitor bank module c, at node i, scenario s

$\hat{q}^{SH}_{i,s}$ Total reactive power injected by the capacitor bank at node i, scenario s

$v_{i,s}$, $v^{SQ}_{i,s}$ Voltage magnitude/its squared value at node i, scenario s

n^{CB}_{i} Integer-valued continuous variable for the number of capacitor banks installed at node i

Binary Variables:

$w^{CB}_{i,c}$ Indicates the installation of capacitor bank module c at node i

w^{I}_{i} Indicates that a capacitor bank is installed at node i

$w^{G}_{i,\varrho}$ Indicates the installation of the dispatchable distributed generation unit of type ϱ at node i

$w^{L}_{ij,a}$ Indicates the installation of conductor of type a on branch ij

$w^{VR}_{ij,a}$ Indicates the installation of the voltage regulator of type a on branch ij

w^{NR}_{ij} Indicates the operating status of branch ij

Integer Variables:

n^{ES}_{i} Indicates the number of energy storage units installed at node i

n^{PV}_{i} Indicates the number of photovoltaic units installed at node i

n^{WT}_{i} Indicates the number of wind turbine units installed at node i

1. Introduction

Distribution system planning (DSP) consists of finding the optimal topological, structural, and physical conditions necessary to ensure that all requirements for electricity delivery in distribution networks can be met with service quality and reliability standards over a planning horizon. Thus, investment in the network, such as the replacement of overloaded conductors, the installation of voltage regulators (VRs), and capacitor banks (CBs) are made in the medium-term planning, while the construction of new feeders and the reinforcement and/or construction of new substations are carried out in long-term planning [1]. There are relevant works in the specialized literature that have focused on making a detailed review of the models and methods proposed to address the DSP problem [2], [3], [4]. According to these works, the new strategies to

approach the planning of modern distribution systems should aim to overcome new challenges resulting from the deployment of renewable technologies encouraged by institutional, social, and environmental policies.

Distribution companies are currently facing new challenges in developing DSP due to the implementation of energy policies aimed at reducing CO_2 emissions in the electricity sector [5]. In this context, carbon tax, carbon cap, and trade in carbon emissions rights are government measures that have been adopted to regulate the environmental impact of industries. The carbon tax is a price-based instrument that defines a fixed tax per tonne of CO_2 emitted [6], the carbon cap is a scheme that imposes a limit to the amount of emissions allowed [7], and the cap-and-trade carbon emissions is a policy that establishes an emissions limit for each emitter and allows a scheme of emissions rights trading for each emitter [8]. Thus, aiming to avoid penalties in the electricity industry, new strategies for DSP must take care not to exceed the CO_2 emissions allowed for the distribution system.

On the other hand, economic subsidies have been implemented to promote the use of renewable energy sources (RES) to achieve a sustainable distribution network [9]. Under this premise, distributed generation (DG) sources based on renewable energy have begun to be massively installed in power distribution systems worldwide to meet the load increase with a low environmental impact. The deployment of renewable DG provides a wide variety of economic, environmental, and technological benefits, however, the operation of these technologies involves a series of uncertainties that significantly hinder DSP [10], [11]. The impact of uncertainty may be partially compensated for with the installation of energy storage (ES) units, which increases the manageability of the grid [12]. Besides, the energy prices at the substation and the demand for electricity are also sources of uncertainties with a relevant impact on DSP, thus, including these uncertain parameters in the optimization method could help to obtain more suitable investment plans.

Given the importance of reducing CO_2 emissions in the electricity industry, modern techniques have emerged for DSP, taking into consideration the installation of low-emissions generation technologies and CO_2 emissions regulation. These approaches are outlined in [13–22].

In [13], a multi-objective particle swarm optimization algorithm is used to solve the problem of sizing and allocating CBs, photovoltaic (PV) generators, and wind turbine (WT) generators in the distribution network. CO_2 emissions have been addressed by minimizing the energy purchased at the substation and energy losses. Uncertainties are addressed by a probabilistic method. A two-stage stochastic programming model for the DSP considering the installation of renewable DG units and CBs is proposed in [14]. The proposed model aims at minimizing carbon emissions tax surpluses while maximizing incentives for the installation of renewable DG units. Uncertainties are addressed through stochastic scenario-based programming. A mixed-integer linear programming (MILP) model for DSP considering the installation of renewable DG units, CBs, and ES units is presented in [15]. CO_2 emissions are controlled by a carbon cap policy. The method proposed is based on a deterministic approach. In [16], an MILP model based on robust optimization is proposed to perform the DSP considering the allocation and sizing of CBs and RESs, the replacement of conductors, and the allocation of VRs. Environmental aspects

are addressed by an energy policy based on a CO_2 emissions cap. In [17], a mixed-integer second-order cone programming (MISOCP) model is proposed for DSP, considering investment several options such as reinforcement of existing substations, replacement of conductors, and allocation and sizing of renewable non-dispatchable and dispatchable DG units. Uncertainties are addressed by stochastic optimization based on scenarios. The proposed approach is aimed at reducing CO_2 emissions through the emissions tax policy. A planning approach similar to the one proposed in [17] is presented in [18]. The main difference is that [18] includes the sizing and allocation of ES units. In [19], a mixed-integer second-order cone programming (MISOCP) model is proposed to manage the installation of network assets, while a low-emission carbon policy was applied to increase the integration of renewable DG sources. The planning strategy includes the installation of ES units, CBs, static compensators, and PV and WT generators. Uncertainties are addressed by robust bi-level optimization. Reference [20] proposes a robust optimization model to solve the DSP, taking into account conventional investment options, as well as the installation of PV and WT units. The objective function of the proposed model minimizes investment and operation costs, besides carbon taxes. Moreover, the demand for electricity is modeled using a voltage-dependent exponential load representation. However, the installation of ES units, and dispatchable renewable DGs, are not considered. In [21], an MILP model is proposed to perform the DSP considering the allocation and sizing of CBs, ES units, and RESs. Environmental aspects are addressed by an energy policy based on CO_2 emissions trading and uncertainties are addressed by robust optimization. Reference [22] proposes a multi-objective approach based on stochastic programming to address the DSP problem. The proposed method seeks to minimize two competing objectives: planning costs and CO_2 emissions. Wind, solar irradiation, and demand uncertainties are modeled using representative scenarios in a MILP formulation. Investments in substations, circuits, and DG allocation are considered. The multi-objective formulation is solved using off-the-shelf commercial software and the well-established ε-constraint method.

Although the deployment of RESs helps to reduce CO_2 emissions in distribution systems, energy-saving strategies may also contribute to the achievement of this objective. Control of nodal voltage magnitudes enables a reduction in energy consumption and active power losses in medium-voltage distribution systems in which loads are predominantly voltage-dependent [23]. Different distribution systems operation studies have used voltage-dependent load models to explore the benefits of this approach. For example, a Volt/VAR control strategy to reduce peak-load and increase energy efficiency in distribution systems is proposed in [24], exploring the conservation voltage reduction (CVR) strategy, which consists of reducing the voltage levels of the network with the objective of reducing the load. The results show that, by considering the load behavior as voltage-dependent, it is possible to obtain several economic and technical benefits, such as a significant reduction in energy consumption and active power losses, as well as the maintenance of the power factor within a specified range. In [25], the authors address the problem of feeders' reconfiguration and allocation of CBs using voltage-dependent load models. The results show that the investment plan obtained without considering voltage-dependent load behavior can be

Table 1: Summary of Literature Review Planning Features

Ref.	Investment alternatives										Voltage dependent load model	Environmental approach	Uncertainty approach	Solution technique
	Replacement of conductors	Modification of the network topology	CBs		VRs		DG units		ES units					
			Size	Location	Size	Location	Size	Location	Size	Location				
[13]	×	×	✓	✓	×	×	✓	✓	×	×	×	Minimize CO_2 emissions	Probabilistic method	Metaheuristic
[14]	×	×	✓	✓	×	×	✓	✓	×	×	×	CO_2 emissions tax and incentives for RESs	Stochastic optimization based on scenarios	MILP
[15]	×	×	✓	✓	×	×	✓	✓	✓	✓	×	CO_2 emissions cap	×	MILP
[16]	✓	×	✓	✓	×	✓	✓	✓	✓	✓	×	CO_2 emissions cap	Robust optimization	MILP
[17]	✓	×	×	×	×	×	✓	✓	×	×	×	CO_2 emissions tax	Stochastic optimization based on scenarios	MISOCP
[18]	✓	×	×	×	×	×	✓	✓	✓	✓	×	CO_2 emissions tax	Stochastic optimization based on scenarios	MISOCP
[19]	×	×	✓	✓	×	×	✓	✓	✓	✓	×	RESs buy obligation	Robust optimization	MISOCP
[20]	✓	×	✓	✓	✓	✓	✓	✓	×	×	✓	CO_2 emissions tax	Robust optimization	MILP
[21]	×	×	✓	✓	×	×	✓	✓	✓	✓	×	CO_2 emissions trading	Robust optimization	MILP
[22]	✓	×	×	×	×	×	✓	✓	×	×	×	Minimize CO_2 emissions	Stochastic optimization based on scenarios	MILP
This Work	✓	✓	✓	✓	✓	✓	✓	✓	✓	✓	✓	CO_2 emissions cap	Stochastic optimization based on scenarios	MILP

infeasible when the solution is evaluated in a complete model with voltage-dependent loads. Despite the benefits discovered in the works mentioned above, voltage-dependent load models are seldom employed in DSP strategies.

Network reconfiguration, on the other hand, is a network operation planning alternative available to achieve significant energy-saving benefits. Network reconfiguration consists of opening and closing switches to modify the network topology with the objective of minimizing active power losses, balancing substation loads [26], improving voltage profiles [27], among others [28]. Despite the benefits of the network reconfiguration, this operation alternative is not often used in medium-term DSP studies.

This work proposes an innovative two-stage stochastic programming model for the medium-term reinforcement planning of active distribution networks, taking into account multiple investment alternatives, network reconfiguration, and CO_2 emissions limit. The advantage of considering multiple alternatives in the DSP problem is that the optimization model can evaluate which network assets are most appropriate to be installed in the distribution system. Unlike [13–22], investment decisions jointly comprise the replacement of overloaded conductors, the installation of voltage control equipment such as CBs and VRs, and the installation of distributed energy resources (DERs), such as dispatchable and non-dispatchable renewable generators, and ES units. As an outstanding feature, the proposed model uses a voltage-dependent representation for the loads and CBs that is more realistic [23] and allows significant energy savings to be achieved. The operation of the distribution system is represented via an ac power flow formulation. Moreover, uncertainties stemming from the demand for electricity, non-dispatchable distributed generation, and energy price at the substation are addressed using scenario-based optimization. The objective function of the proposed model aims to find the investment strategy with the lowest total cost, complying with

the network operating constraints and the CO_2 emissions limit. The model for the DSP is a mixed-integer nonlinear programming (MINLP) problem, which is nonconvex and difficult to solve, but it is converted into an MILP problem by using linearization methods.

Table 1 condenses the main differences between this work and the state-of-art [13–22]. Symbols "✓" and "✖" respectively specify whether a particular feature is considered or not. Therefore, the main contributions of this work are:

1) from a modeling perspective, a new formulation is presented to determine the optimal investment plan for the DSP, improving its effectiveness and reducing the related CO_2 emissions. Uncertainty for renewable generation, energy prices at the substation, and demand for electricity are modeled. Besides that, the load is represented by using a voltage-dependent model, and the network reconfiguration is considered within the network planning options. Modeling the demand as voltage-dependent allows the planning model to modify the network voltage level to reduce the load. In addition, by considering network reconfiguration, the planning model is able to identify the topological conditions necessary for the optimal supply of electrical power. The combination of these two aspects has not yet been considered in the DSP and has a significant impact on the investment and operating costs of the network.
2) from a methodological perspective, a scenario-based programming framework is proposed to model the uncertainty. The resulting deterministic equivalent is formulated as an MINLP problem that is recast to obtain an approximated MILP model that is more realistic and can be successfully solved using commercially available software.

This work contributes to scientific knowledge with two relevant aspects that have not been explored so far to reduce CO_2 emissions from the network. On the one hand, the importance of using a voltage-dependent load model is presented to reduce energy consumption and consequently reduce CO_2 emissions from the network. As shown in the review of the state-of-the-art presented in Table 1, just [15] considers the load as voltage-dependent. However, the mentioned work uses an exponential load model, while the proposed method uses a polynomial load model, also known as the ZIP model. The use of the ZIP load model demands a linearization that is not trivial (linearization of the square of the voltage magnitude). Moreover, [15] does not consider network reconfiguration and energy storage. On the other hand, network reconfiguration has been considered as an operation alternative for reducing the losses of the system, balance the loads, and improve the reliability of the system. This alternative has not been explored to reduce CO_2 emissions from the network. In addition, according to the state-of-the-art presented in Table 1, which shows previous works on medium-term planning for distribution systems, none of these works has considered the reconfiguration of the network as an alternative.

The rest of this work is structured as follows. Section 2 explains how the uncertainties are characterized. Section 3 describes the proposed formulation. Section 4 presents the results obtained for a 69-node test system. Section 5 presents the discussion of the results. Finally, relevant conclusions are drawn in Section 6. Supplementary material is provided in the electronic companion available in [29].

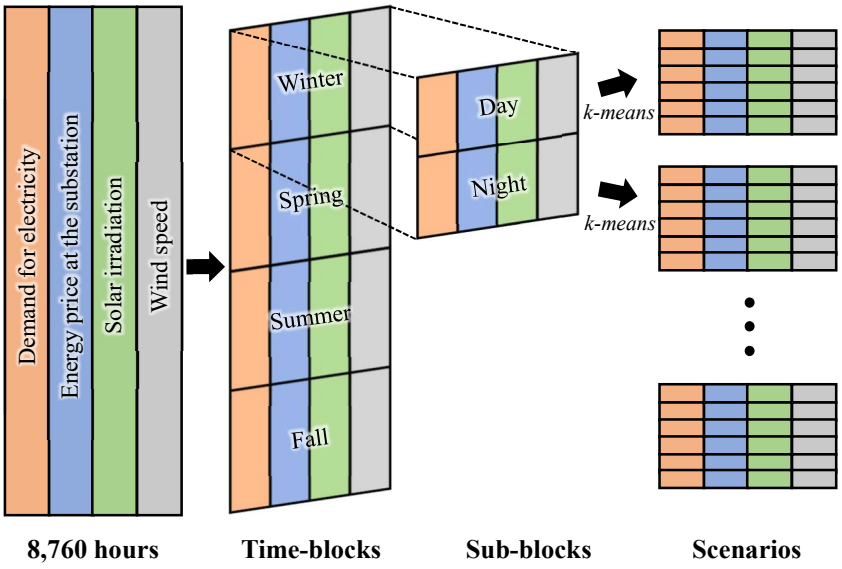

Figure 1: Construction of representative scenarios of the uncertain parameters

2. Uncertainty Modeling

The uncertainties associated with the DSP problem are addressed through scenario-based stochastic optimization [30]. The scenarios are built using historical hourly data of the uncertain parameters throughout a year. Four uncertain parameters are considered in this work: electricity demand, energy price at the substation, solar irradiation, and wind speed.

Due to the complexity of incorporating the 8,760 historical hourly data for each uncertain parameter into the model, the *k-means* method is used to cluster the data into centroids. The role of the *k-means* method is to classify the original data in a certain number of groups according to the similarity and proximity of the data so that the correlation between the original data is guaranteed. The details of the *k-means* method algorithm are given in [31]. Note that the centroids of the group correspond to the mean values of all the data assigned to the group. In this work, the *k-means*++ method from MATLAB's toolbox is used to build the operation scenarios.

Before applying the *k-means* method, the 8,760 data related to the uncertain parameters are divided into four-time blocks according to the seasons of the year (winter, spring, summer, and fall). Each time block is divided into two sub-blocks (day/night) according to the solar irradiation. Finally, the *k-means* method is applied to the information contained in each sub-block to be grouped into k centroids. As a result, a set of $(4 \times 2 \times k)$ scenarios represents the behavior of uncertain parameters throughout the year. Figure 1 illustrates the construction process of the set of scenarios. Note that, the set of scenarios maintains the correlation between the original historical data.

3. Mathematical Formulation of the Problem

The proposed method is formulated considering the following assumptions: (i) based on how the medium-term DSP has usually been developed [15], [16], [20], [21], this work considers a static approach in which all investments in network assets are made at the beginning of the planning horizon; (ii) variations in energy prices, electricity demand, wind speed, and solar irradiation are modeled by a set of scenarios; (iii) the network operates in a radial topology; (iv) Because the medium-voltage three-phase distribution system is considered balanced, its single-phase equivalent can be used to represent it. This assumption is based on common simplifications found in all methods proposed to address medium-voltage DSP [2], [3], [4]. (v) the operation of the distribution system is represented by a linearized AC network model; (vi) the load is modeled as voltage-dependent; (vii) it is taken into account the existence of an environmental policy restricting CO_2 emissions from the network; and (viii) although a centralized planning approach is considered, regardless of DERs ownership, this approach offers useful information about the best investment strategy in terms of environmental and economic factors. Thus, in the scenario that the DERs belong to independent agents, this information can be employed to establish effective incentive strategies, which are outside the scope of this article.

3.1 Objective function

The proposed model's objective function, shown in (1), aims to minimize investment costs and the present value of expected operating costs over an Θ-year planning horizon. The investment cost IC in network assets shown in (2), is composed of seven terms, which represent investments in (i) replacement of overloaded conductors, (ii) VRs, (iii) CBs, where the cost $\mathcal{J}^{CB}$ is used to emphasize that installing CB units at separate nodes is more expensive than installing CB units at the same node, (iv) PV generation units, (v) WT generation units, (vi) dispatchable DG units, and (vii) battery banks. In contrast, the operation cost, OC, shown in (3), consist of : (i) the cost of the energy supplied by the substation, (ii) the generation cost of dispatchable DG units, (iii) the generation cost of PV units, (iv) the generation cost of WT units, and (v) the operating cost of ES units.

$$\text{minimize } IC + OC \tag{1}$$

$$IC = \Theta \left[\sum_{ij \in \Gamma^B} \sum_{a \in \Gamma^L} \mathcal{V}^L_{\dot{a},a} \mathcal{L}_{ij} w^L_{ij,a} + \sum_{ij \in \Gamma^B} \sum_{a \in \Gamma^L} \mathcal{V}^{VR}_a w^{VR}_{ij,a} + \sum_{i \in \Gamma^N} (\mathcal{J}^{CB} w^I_i + \mathcal{V}^{CB} n^{CB}_i) + \sum_{i \in \Gamma^N} \mathcal{V}^{PV} n^{PV}_i + \right.$$
$$\left. \sum_{i \in \Gamma^N} \mathcal{V}^{WT} n^{WT}_i + \sum_{i \in \Gamma^N} \sum_{\varrho \in \Gamma^G} \mathcal{V}^G_\varrho w^G_{i,\varrho} + \sum_{i \in \Gamma^N} \mathcal{V}^{ES} n^{ES}_i \right] \tag{2}$$

$$OC = \sum_{t=1}^{\Theta} \frac{LF_t}{(1+\Pi)^{(t-1)}} \sum_{s \in \Gamma^S} \Delta^T_s \left[\sum_{i \in \Gamma^{SS}} \mathcal{C}^E_s p^{SS}_{i,s} + \sum_{i \in \Gamma^N} \sum_{\varrho \in \Gamma^G} \mathcal{C}^G_\varrho p^G_{i,\varrho,s} + \sum_{i \in \Gamma^N} \mathcal{C}^{PV} p^{PV}_{i,s} + \sum_{i \in \Gamma^N} \mathcal{C}^{WT} p^{WT}_{i,s} + \right.$$
$$\left. \sum_{i \in \Gamma^N} \mathcal{C}^{ES} p^{ES^d}_{i,s} \right] \tag{3}$$

3.2 Power flow modeling

The modeling of the network operation is presented in (4)–(18).

$$\sum_{ki\in\Gamma^B}\sum_{a\in\Gamma^L} p_{ki,a,s} - \sum_{ij\in\Gamma^B}\sum_{a\in\Gamma^L}\left(p_{ij,a,s} + R_a\mathcal{L}_{ij}\imath^{SQ}_{ij,a,s}\right) + p^{SS}_{i,s} + \sum_{\varrho\in\Gamma^G} p^{G}_{i,\varrho,s} + p^{PV}_{i,s} + p^{WT}_{i,s} + p^{ES^d}_{i,s} - p^{ES^c}_{i,s} = \left[\Phi^Z_i\frac{v^{SQ}_{i,s}}{(V^N)^2} + \Phi^I_i\frac{v_{i,s}}{V^N} + \Phi^P_i\right]P^D_{i,s} \quad (4)$$

$$\sum_{ki\in\Gamma^B}\sum_{a\in\Gamma^L} q_{ki,a,s} - \sum_{ij\in\Gamma^B}\sum_{a\in\Gamma^L}\left(q_{ij,a,s} + X_a\mathcal{L}_{ij}\imath^{SQ}_{ij,a,s}\right) + q^{SS}_{i,s} + \hat{q}^{SH}_{i,s} + \sum_{\varrho\in\Gamma^G} q^{G}_{i,\varrho,s} + q^{PV}_{i,s} + q^{WT}_{i,s} = \left[\Upsilon^Z_i\frac{v^{SQ}_{i,s}}{(V^N)^2} + \Upsilon^I_i\frac{v_{i,s}}{V^N} + \Upsilon^P_i\right]Q^D_{i,s} \quad (5)$$

$$\forall i\in\Gamma^N, s\in\Gamma^S$$

$$v_{i,s} = \sqrt{\frac{\overline{V}+\underline{V}}{2}} + \frac{1}{2\sqrt{\frac{\overline{V}+\underline{V}}{2}}}\left(v^{SQ}_{i,s} - \frac{\overline{V}+\underline{V}}{2}\right) \qquad \forall i\in\Gamma^N, s\in\Gamma^S \quad (6)$$

$$v^{SQ}_{i,s} - v^{SQ}_{j,s} + \omega^V_{ij,s} + \vartheta_{ij,s} = \sum_{a\in\Gamma^L}\left[2\mathcal{L}_{ij}(R_a p_{ij,a,s} + X_a q_{ij,a,s}) + Z^2_a\mathcal{L}^2_{ij}\imath^{SQ}_{ij,a,s}\right] \quad (7)$$

$$\forall ij\in\Gamma^B, a\in\Gamma^L, s\in\Gamma^S$$

$$\left|\vartheta_{ij,s}\right| \le \left(\overline{V}^2 - \underline{V}^2\right)(1 - w^{NR}_{ij}) \qquad \forall ij\in\Gamma^B, a\in\Gamma^L, s\in\Gamma^S \quad (8)$$

$$\tilde{V}^2_{j,s}\hat{\imath}^{SQ}_{ij,s} = \sum_{\psi=1}^{\Psi}\mathcal{M}^{\hat{S}}_{ij,\psi}\left(\delta^{\hat{p}}_{ij,\psi,s} + \delta^{\hat{q}}_{ij,\psi,s}\right) \qquad \forall ij\in\Gamma^B, s\in\Gamma^S \quad (9)$$

$$\hat{p}_{ij,s} = \hat{p}^{+}_{ij,s} - \hat{p}^{-}_{ij,s} \qquad \forall ij\in\Gamma^B, s\in\Gamma^S \quad (10)$$

$$\hat{p}^{+}_{ij,s} + \hat{p}^{-}_{ij,s} = \sum_{\psi=1}^{\Psi}\delta^{\hat{p}}_{ij,\psi,s} \qquad \forall ij\in\Gamma^B, s\in\Gamma^S \quad (11)$$

$$0 \le \delta^{\hat{p}}_{ij,\psi,s} \le \overline{\Delta}^{\hat{S}}_{ij} \qquad \forall ij\in\Gamma^B, \psi\in\{1,\cdots,\Psi\}, s\in\Gamma^S \quad (12)$$

$$\hat{q}_{ij,s} = \hat{q}^{+}_{ij,s} - \hat{q}^{-}_{ij,s} \qquad \forall ij\in\Gamma^B, s\in\Gamma^S \quad (13)$$

$$\hat{q}^{+}_{ij,s} + \hat{q}^{-}_{ij,s} = \sum_{\psi=1}^{\Psi}\delta^{\hat{q}}_{ij,\psi,s} \qquad \forall ij\in\Gamma^B, s\in\Gamma^S \quad (14)$$

$$0 \le \delta^{\hat{q}}_{ij,\psi,s} \le \overline{\Delta}^{\hat{S}}_{ij} \qquad \forall ij\in\Gamma^B, \psi\in\{1,\cdots,\Psi\}, s\in\Gamma^S \quad (15)$$

$$\hat{\imath}^{SQ}_{ij,s} = \sum_{a\in\Gamma^L}\imath^{SQ}_{ij,a,s} \qquad \forall ij\in\Gamma^B, s\in\Gamma^S \quad (16)$$

$$\hat{p}_{ij,s} = \sum_{a\in\Gamma^L} p_{ij,a,s} \qquad \forall ij\in\Gamma^B, s\in\Gamma^S \quad (17)$$

$$\hat{q}_{ij,s} = \sum_{a\in\Gamma^L} q_{ij,a,s} \qquad \forall ij\in\Gamma^B, s\in\Gamma^S \quad (18)$$

Two variable substitutions are performed to convert the original MINLP formulation for the DSP problem into an MILP model, i.e., $v^2_{i,s}$ is replaced with the linear term $v^{SQ}_{i,s}$, and $\imath^2_{ij,a,}$ is replaced with the linear term $\imath^{SQ}_{ij,a,s}$.

The active and reactive power balances, representing the application of Kirchhoff's current law to the system, are shown in (4) and (5), which consider the polynomial ZIP load model to represent the voltage-dependent behavior of the loads. Constant impedance (Z), constant current (I), and constant power (P) components are used in this representation to model the load as a function of the voltage magnitude, according to the participation parameters Φ and Υ [32].

Constraint (6) is the expansion of $v_{i,s}^2$ employing a Taylor series at $(\overline{V}+\underline{V})/2$. The variable $v_{i,s}$ is employed in the ZIP model, and the maximum error of this linearization occurs for $v_{i,s}=\underline{V}$. Thus, for $\underline{V}=0.95$ p.u., this error is 0.13%.

Constraints (7)–(9) represent the application of Kirchhoff's voltage law to the system. Constraint (7) calculates the difference of the squared values of the voltage magnitudes at the terminal nodes of a branch according to the active and reactive power flows and the current magnitude on the branch. The variable $\omega_{ij,s}^V$ is used to model the operation of VRs, while $\vartheta_{ij,s}$ is a slack variable, limited in (8) according to the state of the switch of the branch represented by w_{ij}^{NR}. Constraint (9) is a piecewise linearization of the original nonlinear constraint $v_{j,s}^{SQ}\hat{\imath}_{ij,s}^{SQ}=\hat{p}_{ij,s}^2+\hat{q}_{ij,s}^2$, in which $v_{j,s}^{SQ}$ is replaced with an estimate of the voltage magnitude $\tilde{V}_{i,s}$, and the quadratic terms $\hat{p}_{ij,s}^2$ and $\hat{q}_{ij,s}^2$ are approximated employing a piecewise linearization, as presented in (10)–(15). In (9)–(15), the length of each block of the linearization is $\overline{\Delta}_{ij}^{\hat{S}}=\overline{V}\max\limits_{a\in\Gamma^L}\overline{I}_a/\Psi$, and the slope of each block is $\mathcal{M}_{ij,1}^{\hat{S}}=(5/6)\overline{\Delta}_{ij}^{\hat{S}}$ and $\mathcal{M}_{ij,\psi}^{\hat{S}}=(2\psi-1)\overline{\Delta}_{ij}^{\hat{S}}$ for $\psi>1$.

Constraints (16)–(18) calculate the total power flow and current in each branch as the sum of the power flows and currents in each conductor of each branch. Note that only one conductor can be selected for each branch, as presented in (23).

3.3 Operational limits

The network's operational limits are presented in (19)–(22).

$$\underline{V}^2\leq v_{i,s}^{SQ}\leq\overline{V}^2 \qquad \forall i\in\Gamma^N, s\in\Gamma^S \tag{19}$$

$$0\leq p_{i,s}^{SS}\leq\overline{S}_i^{SS} \qquad \forall i\in\Gamma^{SS}, s\in\Gamma^S \tag{20}$$

$$\left|q_{i,s}^{SS}\right|\leq\overline{S}_i^{SS} \qquad \forall i\in\Gamma^{SS}, s\in\Gamma^S \tag{21}$$

$$\left|q_{i,s}^{SS}\right|\leq\sqrt{2}\ \overline{S}_i^{SS}-p_{i,s}^{SS} \qquad \forall i\in\Gamma^{SS}, s\in\Gamma^S \tag{22}$$

Constraint (19) presents the limits for the voltage magnitudes at the nodes. The set of constraints (20)–(22) represent the power injection limits of the substations, which consider a linearization for the original quadratic constraint $(p_{i,s}^{SS})^2+(q_{i,s}^{SS})^2\leq\left(\overline{S}_i^{SS}\right)^2$ with $p_{i,s}^{SS}\geq 0$.

3.4 Constraints for investment in conductors

Constraints (23) and (24) are associated with the investment and operational limits of the conductors.

$$\sum_{a\in\Gamma^L}w_{ij,a}^L\leq 1 \qquad \forall ij\in\Gamma^B \tag{23}$$

$$0\leq\imath_{ij,a,s}^{SQ}\leq\overline{I}_a^2 w_{ij,a}^L \qquad \forall ij\in\Gamma^B, a\in\Gamma^L, s\in\Gamma^S \tag{24}$$

Constraint (23) guarantees that at most a single type of conductor is selected for each branch. The currents on the branches are limited by (24), according to the type of conductor installed.

3.5 Constraints for investment in VRs

The operation of the VRs is defined in (25) and (26), while (27) and (28) are investment constraints.

$$|\omega^{V}_{ij,s}| \leq K^{VR}(K^{VR}+2)v^{SQ}_{i,s} \qquad \forall ij \in \Gamma^{B}, s \in \Gamma^{S} \tag{25}$$

$$|\omega^{V}_{ij,s}| \leq \sum_{a \in \Gamma^{L}} w^{VR}_{ij,a} K^{VR}(K^{VR}+2)\overline{V}^{2} \qquad \forall ij \in \Gamma^{B}, s \in \Gamma^{S} \tag{26}$$

$$w^{VR}_{ij,a} \leq w^{L}_{ij,a} \qquad \forall ij \in \Gamma^{B}, a \in \Gamma^{L}, s \in \Gamma^{S} \tag{27}$$

$$\sum_{ij \in \Gamma^{B}} \sum_{a \in \Gamma^{L}} w^{VR}_{ij,a} \leq \overline{\mathcal{N}}^{VR} \tag{28}$$

Constraint (25) presents the limit for $\omega^{V}_{ij,s}$ according to the maximum regulation of the VR, while (26) calculates the difference between the square of the voltage magnitudes across a VR, $\omega^{V}_{ij,s}$, in accordance with the binary investment variable $w^{VR}_{ij,a}$. Constraint (27) requires that a VR of type a must only be installed on a branch with a conductor of type a, given that the current capacity of the VR of type a matches the current capacity of the conductor of type a, while (28) limits the number of VRs installed in the system.

3.6 Constraints for investment in CBs

Constraints (29)–(31) are related to the operation and (32)–(34) are related to the investments in CBs.

$$\hat{q}^{SH}_{i,s} = \sum_{c=1}^{\overline{N}^{CB}_{i}} q^{SH}_{i,c,s} \qquad \forall i \in \Gamma^{N}, s \in \Gamma^{S} \tag{29}$$

$$-\overline{V}^{2}\mathcal{B}^{CB}(1-w^{CB}_{i,c}) \leq q^{SH}_{i,c,s} - \mathcal{B}^{CB}v^{SQ}_{i,s} \leq -\underline{V}^{2}\mathcal{B}^{CB}(1-w^{CB}_{i,c}) \qquad \forall i \in \Gamma^{N}, c \in \left\{1, \cdots, \overline{N}^{CB}_{i}\right\}, s \in \Gamma^{S} \tag{30}$$

$$\underline{V}^{2}\mathcal{B}^{CB}w^{CB}_{i,c} \leq q^{SH}_{i,c,s} \leq \overline{V}^{2}\mathcal{B}^{CB}w^{CB}_{i,c} \qquad \forall i \in \Gamma^{N}, c \in \left\{1, \cdots, \overline{N}^{CB}_{i}\right\}, s \in \Gamma^{S} \tag{31}$$

$$\sum_{c=1}^{\overline{N}^{CB}_{i}} w^{CB}_{i,c} = n^{CB}_{i} \qquad \forall i \in \Gamma^{N} \tag{32}$$

$$0 \leq n^{CB}_{i} \leq \overline{N}^{CB}_{i} w^{I}_{i} \qquad \forall i \in \Gamma^{N} \tag{33}$$

$$\sum_{i \in \Gamma^{N}} w^{I}_{i} \leq \overline{\mathcal{N}}^{CB} \tag{34}$$

The total reactive power injected by the CB at node i is calculated in (29) as the sum of the contribution of each module, while (30) and (31) calculate the reactive power injected by each CB module according to the values of the investment variables and the voltage magnitude at the installation node for each scenario. Note that if $w^{CB}_{i,c} = 0$, then $q^{SH}_{i,c,s} = 0$ in (31), whereas if $w^{CB}_{i,c} = 1$, then $q^{SH}_{i,c,s} = \mathcal{B}^{CB}v^{SQ}_{i,s}$ in (30). The total number of CB modules installed at each node is calculated in (32), the number of CB modules that can be installed at each node is limited in (33), and the number of CBs that can be installed in the system is limited in (34).

3.7 Constraints for investment in dispatchable DG units

The operation and investment in DGs are defined in (35)–(41).

$$0 \leq p^{G}_{i,\varrho,s} \leq \overline{S}^{G}_{\varrho} w^{G}_{i,\varrho} \qquad \forall i \in \Gamma^{N}, \varrho \in \Gamma^{G}, s \in \Gamma^{S} \tag{35}$$

$$\left|q^G_{i,\varrho,s}\right| \le \overline{S}^G_{\varrho} w^G_{i,\varrho} \qquad \forall i \in \Gamma^N, \varrho \in \Gamma^G, s \in \Gamma^S \tag{36}$$

$$\left|q^G_{i,\varrho,s}\right| \le \sqrt{2}\ \overline{S}^G_{\varrho} w^G_{i,\varrho} - p^G_{i,\varrho,s} \qquad \forall i \in \Gamma^N, \varrho \in \Gamma^G, s \in \Gamma^S \tag{37}$$

$$-p^G_{i,\varrho,s} \tan(\cos^{-1}(\underline{PF}^G_{\varrho})) \le q^G_{i,\varrho,s} \le p^G_{i,\varrho,s} \tan\left(\cos^{-1}\left(\overline{PF}^G_{\varrho}\right)\right) \qquad \forall i \in \Gamma^N, \varrho \in \Gamma^G, s \in \Gamma^S \tag{38}$$

$$\sum_{\varrho \in \Gamma^G} w^G_{i,\varrho} \le 1 \qquad \forall i \in \Gamma^N \tag{39}$$

$$0 \le w^G_{i,\varrho} \le \overline{\mathcal{W}}^G_i \qquad \forall i \in \Gamma^N, \varrho \in \Gamma^G \tag{40}$$

$$\sum_{i \in \Gamma^N} \sum_{\varrho \in \Gamma^G} w^G_{i,\varrho} \le \overline{\mathcal{N}}^G \tag{41}$$

The active and reactive power limits of dispatchable DG units are established in constraints (35)–(38), which represent a linearization of the capability curve of a synchronous machine. The power factor limits of the generator are shown in (38). Constraint (39) determines that at most one type of dispatchable DG can be installed at node i, while (40) defines the candidate nodes for the installation of a dispatchable DG, according to the binary parameter $\overline{\mathcal{W}}^G_i$. The number of dispatchable DG units that can be installed in the network is limited in (41).

3.8 Constraints for investment in PV and WT units

Constraints (42)–(47) represent the installation and operation of PV units.

$$0 \le p^{PV}_{i,s} \le \overline{S}^{PV} \mathcal{F}^{PV}_s n^{PV}_i \qquad \forall i \in \Gamma^N, s \in \Gamma^S \tag{42}$$

$$\left|q^{PV}_{i,s}\right| \le \overline{S}^{PV} n^{PV}_i \qquad \forall i \in \Gamma^N, s \in \Gamma^S \tag{43}$$

$$\left|q^{PV}_{i,s}\right| \le \sqrt{2}\ \overline{S}^{PV} n^{PV}_i - p^{PV}_{i,s} \qquad \forall i \in \Gamma^N, s \in \Gamma^S \tag{44}$$

$$-p^{PV}_{i,s} \tan(\cos^{-1}(\underline{PF}^{PV})) \le q^{PV}_{i,s} \le p^{PV}_{i,s} \tan\left(\cos^{-1}\left(\overline{PF}^{PV}\right)\right) \qquad \forall i \in \Gamma^N, s \in \Gamma^S \tag{45}$$

$$0 \le n^{PV}_i \le \overline{N}^{PV}_i \qquad \forall i \in \Gamma^N \tag{46}$$

$$\sum_{i \in \Gamma^N} n^{PV}_i \le \overline{\mathcal{N}}^{PV} \tag{47}$$

The active and reactive power injections of PV units at node i, scenario s, are limited by (42)–(45), according to the number of PV units installed at the node and the generation factor of the scenario. The power factor limits for the operation of the power converter of the PV units are considered in (45). The number of PV units that can be installed at each node i is limited in (46) limits and the number of PV units that can be installed in the entire system is limited in (47).

The installation and operation of WT units are represented in constraints (48)–(53), which are similar to (42)–(47).

$$0 \le p^{WT}_{i,s} \le \overline{S}^{WT} \mathcal{F}^{WT}_s n^{WT}_i \qquad \forall i \in \Gamma^N, s \in \Gamma^S \tag{48}$$

$$\left|q^{WT}_{i,s}\right| \le \overline{S}^{WT} n^{WT}_i \qquad \forall i \in \Gamma^N, s \in \Gamma^S \tag{49}$$

$$\left|q^{WT}_{i,s}\right| \le \sqrt{2}\ \overline{S}^{WT} n^{WT}_i - p^{WT}_{i,s} \qquad \forall i \in \Gamma^N, s \in \Gamma^S \tag{50}$$

$$-p^{WT}_{i,s} \tan(\cos^{-1}(\underline{PF}^{WT})) \le q^{WT}_{i,s} \le p^{WT}_{i,s} \tan\left(\cos^{-1}\left(\overline{PF}^{WT}\right)\right) \qquad \forall i \in \Gamma^N, s \in \Gamma^S \tag{51}$$

$$0 \le n^{WT}_i \le \overline{N}^{WT}_i \qquad \forall i \in \Gamma^N \tag{52}$$

$$\sum_{i\in\Gamma_i^N} n_i^{WT} \leq \overline{\mathcal{N}}^{WT} \tag{53}$$

3.9 Constraints for investment in ES units

Constraints (54)–(58) represent the installation and operation of ES units.

$$p_{i,s}^{ES^c} \leq \overline{P}^{ES} n_i^{ES} \qquad \forall i \in \Gamma^N, s \in \Gamma^S \tag{54}$$

$$p_{i,s}^{ES^d} \leq \overline{P}^{ES} n_i^{ES} \qquad \forall i \in \Gamma^N, s \in \Gamma^S \tag{55}$$

$$\sum_{s\in\Gamma^S|\Omega_s=b} \Delta_s^T \left[\mathcal{X}^{ES^c} p_{i,s}^{ES^c} - \left(\frac{1}{\mathcal{X}^{ES^d}}\right) p_{i,s}^{ES^d}\right] = 0 \qquad \forall i \in \Gamma^N, b \in \{1,\cdots,4\} \tag{56}$$

$$0 \leq n_i^{ES} \leq \overline{N}_i^{ES} \qquad \forall i \in \Gamma^N \tag{57}$$

$$\sum_{i\in\Gamma^N} n_i^{ES} \leq \overline{\mathcal{N}}^{ES} \tag{58}$$

The charging and discharging operations of the ES units are constrained by (54) and (55), respectively. The transition function of ES units to be accomplished at each block of scenarios, in which each block represents a season of the year, is shown in (56), requiring that the energy can only be exchanged among the scenarios of the same block. The number of ES units that can be installed at node i is restricted in (57) and the number of ES units that can be installed in the entire system is limited in (58).

3.10 Network reconfiguration formulation

The formulation of the network reconfiguration is shown in (59)–(66).

$$|p_{ij,a,s}| \leq \overline{VI}_a w_{ij}^{NR} \qquad \forall ij \in \Gamma^B, a \in \Gamma^L, s \in \Gamma^S \tag{59}$$

$$|q_{ij,a,s}| \leq \overline{VI}_a w_{ij}^{NR} \qquad \forall ij \in \Gamma^B, a \in \Gamma^L, s \in \Gamma^S \tag{60}$$

$$0 \leq i_{ij,a,s}^{SQ} \leq \overline{I}_a^2 w_{ij}^{NR} \qquad \forall ij \in \Gamma^B, a \in \Gamma^L, s \in \Gamma^S \tag{61}$$

$$\sum_{ij\in\Gamma^B} w_{ij}^{NR} = |\Gamma^N| - |\Gamma^{SS}| \tag{62}$$

$$\sum_{ki\in\Gamma^B} f_{ki} - \sum_{ij\in\Gamma^B} f_{ij} + g_i = 1 \qquad \forall i \in \Gamma^N \tag{63}$$

$$0 \leq g_i \leq |\Gamma^N| \qquad \forall i \in \Gamma^{SS} \tag{64}$$

$$g_i = 0 \qquad \forall i \in \{\Gamma^N - \Gamma^{SS}\} \tag{65}$$

$$|f_{ij}| \leq (|\Gamma^N| - 1)\ w_{ij}^{NR} \qquad \forall ij \in \Gamma^B \tag{66}$$

Constraints (59) and (60) are, respectively, the active and reactive power flows limits on the conductors according to the operating statuses of the branches, while (61) limits the currents on the branches. Constraints (62)–(66) guarantee that the system operation is radial [33]. Note that constraint (62) is a necessary condition for radiality, while constraints (63)–(66) ensure the connectivity of the system. Constraint (63) represents a fictitious balance in the system, constraint (64) is the limit for the fictitious generation at the substation nodes, constraint (65) fixes the fictitious generation in zero at the demand nodes, and constraint (66) limits the fictitious flow f_{ij} on the branches according to their operating statuses. These constraints require the existence of a path from a substation to each demand node, therefore, ensuring the connectivity of the system.

3.11 CO_2 emissions limit

The limit of CO_2 emissions is modeled by (67).

$$\sum_{i\in\Gamma^N}\sum_{s\in\Gamma^S}\Delta_s^T\left(\mathcal{E}^{SS}p_{i,s}^{SS}+\sum_{\varrho\in\Gamma^G}\mathcal{E}_{\varrho}^{G}p_{i,\varrho,s}^{G}+\mathcal{E}^{PV}p_{i,s}^{PV}+\mathcal{E}^{WT}p_{i,s}^{WT}\right)\leq\overline{\Lambda} \tag{67}$$

Constraint (67) limits the total annual CO_2 emissions from the distribution system to a maximum $\overline{\Lambda}$.

3.12 Two-stage stochastic programming model

The proposed model for the medium-term planning of active distribution networks (1)–(67) is a two-stage stochastic mixed-integer linear program. In the decision-making process of two-stage optimization problems, two different types of decisions are characterized:

1) First-stage or here-and-now decisions: These decisions are made before carrying out the stochastic process since the variables that represent decisions here-and-now do not depend on uncertainties. In the DSP problem, the here-and-now decision variables are those that are related to network reconfiguration, investment in substitution of overloaded conductors, and the installation of CBs, VRs, PVs, WTs, and ES units.
2) Second-stage or wait-and-see decisions: These decisions are made after knowing the real value of the stochastic process, as these decisions depend on uncertainties. In the DSP problem, the wait-and-see decision variables are those that are related to the operation of the system, which are used in the calculation of the expected cost of operating the system, as well as CO_2 emissions. All variables with an index s are second-stage variables.

A more extensive and detailed explanation of how the two-stage optimization problems are modeled and solved can be found in [30]. Moreover, it should be clarified that the model (1)–(67) can be directly solved by off-the-shelf optimization software based on the branch-and-cut algorithm.

4. Tests and Results

The proposed model was written in AMPL [34] and solved with CPLEX v20.1.0.0 [35], with default settings, on a computer with a 3.20 GHz Intel® Core™ i7–8700 processor and 32 GB of RAM. Two distribution systems were used to test the proposed model: a 69-node test system and a 2313-node real system.

4.1 69-node distribution system

The 69-node distribution system from [36] was adapted to test the proposed model. Figure 2 shows the network topology of the system. The system consists of one substation node, 73 branches, two transfer nodes, and 66 load nodes. All

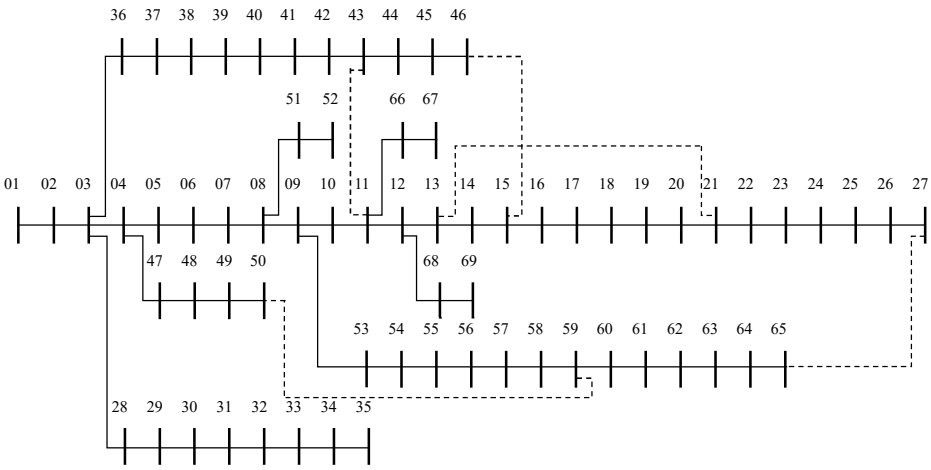

Figure 2: Initial configuration of the 69-node system

branches have conductors of type I and in the initial configuration, branches 11-43, 13-21, 15-46, 27-65, and 50-59 are open. The lower and upper voltage magnitude limits are 0.95 p.u. and 1.05 p.u., respectively. The nominal voltage of the system is 12.66 kV. The planning horizon is five years. The demand is estimated based on an annual average growth of 3%. The number of centroids is $k = 6$, thereby obtaining 48 operation scenarios. It is considered an annual interest rate of 10%. The number of blocks used in the piecewise linearization is $\Psi = 10$. Complete information for the 69-node distribution system is presented in [29].

Four case studies have been considered to demonstrate the applicability and significance of the proposed model. In Case A-I, DSP is developed without considering network reconfiguration and using a constant power load model. Case A-II is similar to Case A-I, the only difference is that, in Case A-II, network reconfiguration is considered. In Case A-III, DSP is developed without considering network reconfiguration, and using the voltage-dependent load model. Finally, in Case A-IV, both network reconfiguration and the voltage-dependent load model are jointly considered. The technical and economic details of the investment alternatives considered in the four case studies are available in the electronic companion available in [29].

The computational times to solve Cases A-I until A-IV are 0.90 h, 4.47 h, 0.92 h, and 28.62 h, respectively.

For the four case studies, we consider that the planning strategy is based on an energy policy that limits the CO_2 emissions to 7,000 tonnes. This value is chosen on a random basis because the network is illustrative. However, for a real case study, the current legislation of the corresponding country can be considered. Table 2 provides information about costs and CO_2 emissions for the solutions attained for each case. Besides, Table 3 shows the investment strategies for the four cases. Operational results for the 69-node distribution system are presented in [29].

For Case A-I, in which network reconfiguration is not considered and the demand is modeled as constant power load, the proposed method has found a planning strategy with a total investment cost of US$ 4,862.59×10^3. The investment

Table 2: Overview of the Solutions for the 69-Node System

Results		Case A-I	Case A-II	Case A-III	Case A-IV
Investment cost ($\times 10^3$ US$)	Conductors	11.68	2.54	20.03	5.69
	CBs	8.85	5.90	11.80	5.90
	VRs	3.74	–	22.43	22.43
	Biomass DG units	214.00	214.00	214.00	214.00
	PV units	367.25	339.00	197.75	56.50
	WT units	3,957.07	3,957.07	3,507.40	3,597.33
	ES units	300.00	300.00	280.00	300.00
Total investment cost ($\times 10^3$ US$)		4,862.59	4,818.51	4,253.41	4,201.85
Total operation cost ($\times 10^3$ US$)		6,381.66	6,372.39	6,111.52	6,107.66
Total cost ($\times 10^3$ US$)		11,244.25	11,190.90	10,364.93	10,309.51
Minimum voltage magnitude (p.u.)		0.95	0.95	0.95	0.95
Maximum voltage magnitude (p.u.)		1.05	1.05	0.99	0.99
Annual CO_2 emissions ($\times 10^3$ tonnes)		7.00	7.00	7.00	7.00

Table 3: Investments Plans for the 69-Node System

Investment option	Case A-I	Case A-II	Case A-III	Case A-IV
Replacement of conductors (branch ij, type)	01-02, II; 02-03, II; 03-04, II 04-05, II; 05-06, II; 06-07, II 07-08, II; 08-09, II	01-02, II; 02-03, II; 11-12, II	01-02, II; 02-03, II; 03-04, II 04-05, II; 05-06, II; 06-07, II 07-08, II; 08-09, II; 55-56, II 58-59, II; 59-60, II; 60-61, II	01-02, II; 02-03, II; 03-04, II 04-05, II; 59-60, II
Network reconfiguration (open branches)	–	08-09; 09-10; 14-15 22-23; 43-44	–	14-15; 22-23; 40-41 43-44; 56-57
VRs (branch ij, type)	10-11, I	–	04-10, I; 19-20, I; 03-28, I 03-36, I; 04-47, I; 09-53, I	06-07, II 09-10, I; 19-20, I 03-28, I; 03-36, I; 60-61, I
CBs (node i, number of units)	14, 1; 24, 1; 64, 1	14, 1; 64, 1	14, 1; 24, 1; 45, 1; 57, 1	14, 1; 24, 1
Biomass DG units (node i, type)	16, I; 31, I; 41, I 49, I; 58, I; 62, I	16, I; 31, I; 41, I 49, I; 58, I; 62, I	16, I; 31, I; 41, I 49, I; 58, I; 62, I	16, I; 31, I; 41, I 49, I; 58, I; 62, I
WT units (node i, number of units)	17, 17; 34, 10; 56, 10; 63, 7	17, 15; 34, 9; 56, 7; 63, 13	17, 15; 34, 7; 56, 11; 63, 6	17, 13; 34, 7; 56, 7; 63, 13
PV units (node i, number of units)	19, 3; 26, 3; 43, 3 60, 3; 64, 1	19, 3; 26, 3 43, 3; 60, 3	19, 2; 26, 3; 43, 2	19, 2
ES units (node i, number of units)	16, 3; 17, 3; 19, 3; 26, 3; 33, 2 34, 3; 41, 3; 43, 3; 60, 3; 64, 3	16, 3; 17, 3; 19, 3; 26, 3; 33, 2 34, 3; 41, 3; 43, 3; 60, 3; 64, 3	16, 3; 17, 3; 19, 3; 26, 3; 33, 2 34, 3; 41, 3; 43, 1; 60, 3; 64, 3	16, 3; 17, 3; 19, 3; 26, 3; 33, 2 34, 3; 41, 3; 43, 3; 60, 3; 64, 3

Table 4: Evaluation of the Operation for the Plans of Cases A-I and A-II Considering the Demand Modeled as Voltage-Dependent Load for the 69-Node System

	Case A-I		Case A-II	
	Demand modeled as constant power load	Demand modeled as voltage-dependent load	Demand modeled as constant power load	Demand modeled as voltage-dependent load
Total investment cost ($\times 10^3$ US$)	4,862.59	4,862.59	4,818.51	4,818.51
Total operation cost ($\times 10^3$ US$)	6,381.66	5,835.20	6,372.39	5,765.33
Total cost ($\times 10^3$ US$)	11,244.25	10,697.82	11,190.90	10,583.84
Minimum voltage magnitude (p.u.)	0.95	0.95	0.95	0.95
Maximum voltage magnitude (p.u.)	1.05	1.05	1.05	1.03
Annual CO_2 emissions (10^3 tonnes)	7.00	6.34	7.00	6.23

plan consists of replacing the conductors of branches 01-02, 02-03, 03-04, 04-05, 05-06, 06-07, 07-08, and 08-09 with conductors of type II; installing a 300 kVAr CB unit at nodes 14, 24, and 64; installing one VR of type I on branch 10-11; installing a biomass DG unit of type I at nodes 16, 31, 41, 49, 58, and 62; installing 17 400 kW WT units at node 17, ten 400

kW WT units at node 34, ten 400 kW WT units at node 56, and seven 400 kW WT units at node 63; installing three 100 kW PV units at nodes 19, 26, 43, and 60 and one 100 kW PV unit at node 64; installing three 50 kW ES units at nodes 16, 17, 19, 26, 34, 41, 43, 60, and 64 and two 50 kW ES units at node 33. Moreover, the proposed model shows that, with this investment plan, the network operating cost is US$ 6,381.66×10^3, thus, the total expected cost considering the conditions of Case A-I is US$ 11,244.25×10^3.

For Case A-II, in which network reconfiguration is considered and the demand is represented using a constant power load model, the proposed method has found an investment plan with a cost of US$ 4,818.51×10^3. The investment plan suggests replacing the conductors of branches 01-02, 02-03, and 11-12 with conductors of type II; open branches 08-09, 09-10, 14-15, 22-23, and 43-44; installing one 300 kVAr CB unit at nodes 14 and 64; installing one biomass DG unit of type I at nodes 16, 31, 41, 49, 58, and 62, installing 15 400 kW WT units at node 17, nine 400 kW WT units at node 34, seven 400 kW WT units at node 56, and 13 400 kW WT units at node 63; installing three 100 kW PV units at nodes 19, 26, 43, and 60; installing three 50 kW ES units at nodes 16, 17, 19, 26, 34, 41, 43, 60, and 64 and two 50 kW ES units at node 33. For the investment plan found, the network operating cost is US$ 6,372.39×10^3. Thus, the total expected cost under the conditions of Case A-II is US$ 11,190.90×10^3.

For Case A-III, in which network reconfiguration is disregarded and the demand is modeled as voltage-dependent load, the proposed method has found a plan with a total investment cost of US$ 4,253.41×10^3. The planning strategy consists of replacing the conductors of branches 01-02, 02-03, 03-04, 04-05, 05-06, 06-07, 07-08, 08-09, 55-56, 58-59, 59-60, and 60-61 with conductors of type II; installing one 300 kVAr CB unit at nodes 14, 24, 45, and 57; installing one VR of type I on branches 04-10, 19-20, 03-28, 03-36, 04-47, and 09-53; installing one biomass DG unit of type I at nodes 16, 31, 41, 49, 58, and 62; installing 15 400 kW WT units at node 17, seven 400 kW WT units at node 34, eleven 400 kW WT units at node 56, and six 400 kW WT units at node 63; installing two 100 kW PV units at nodes 19, and 43, and three 100 kW PV units at node 26; installing three 50 kW ES units at nodes 16, 17, 19, 26, 34, 41, 43, 60, and 64 and two 50 kW ES units at node 32; installing three 50 kW ES units at nodes 16, 17, 19, 26, 34, 41, 60, and 64, two 50 kW ES units at node 32 and one 50 kW ES units at node 43. Furthermore, the proposed model calculated that, with this investment, there will be a network operating cost of US$ 6,111.52×10^3, so the total expected cost considering the conditions of Case A-III for the 5-year planning horizon is US$ 10,364.93×10^3.

For Case A-IV, in which network reconfiguration is considered and the demand is represented by the voltage-dependent load model, the proposed method has found an investment plan with a cost of US$ 4,201.85. The investment plan suggests replacing the conductors of branches 01-02, 02-03, 03-04, 04-05, and 59-60 with conductors of type II; open branches 14-15, 22-23, 40-41, 43-44, and 56-57; installing one 300 kVAr CB unit at nodes 14 and 24; installing one VR of type I on branches 06-07, 09-10, 19-20, 03-28, 03-36, and 60-61; installing one biomass DG unit of type I at nodes 16, 31, 41, 49, 58, and 62; installing 13 400 kW WT units at node 17, seven 400 kW WT units at node 34, seven 400 kW WT units

Table 5: Total Planning Costs as a Function of the Number of Operating Conditions for the 69-Node System

Number of centroids	Number of operation scenarios	Total cost $\times 10^3$ US$	Absolute value of the difference in (%)	CPU time (h)
1	8	10,010.53	2.90%	1.59
3	24	10,316.15	0.06%	7.82
6	48	10,309.51	–	28.62
12	96	10,325.59	0.16%	45.83
24	192	10,381.25	0.70%	97.48
36	288	10,394.11	0.82%	118.41
48	384	10,393.55	0.82%	175.72

at node 56, and 13 400 kW WT units at node 63; installing two 100 kW PV units at node 19; installing three 50 kW ES units at nodes 16, 17, 19, 26, 34, 41, 43, 60, and 64 and two 50 kW ES units at node 33. For the investment plan found, the operating cost of the network is US$ 6,107.66. Therefore, the total expected cost under the conditions of Case A-IV is US$ 10,309.51.

The investment plans obtained for Cases A-I and A-II, in which the demands were modeled as constant power loads, were evaluated using the voltage-dependent load model to compare the variations in the network operating costs. For both cases, the investment plans are fixed, while the voltage control at the substation and the redispatch of the DERs is allowed. The results of these comparisons are shown in Table 4. By analyzing Table 4, it is possible to verify that, the total costs for Cases A-I and A-II are 3.21% and 2.74% higher than the total costs for the solutions of Cases A-III and A-IV, respectively, which are presented in Table 2.

Finally, in order to demonstrate and justify the effectiveness of using 48 operating scenarios, other simulations were performed for Case A-IV, with different numbers of operating scenarios. Table 5 shows the absolute values of the differences between the total costs with 8, 24, 48, 96, 192, 288, and 384 scenarios in relation to the total cost of the solution obtained with 48 scenarios (base case). Note that, by considering larger numbers of scenarios, the computational time to solve the problem grows rapidly, with almost no change in the total cost. Therefore, it can be concluded that the selected number of scenarios is suitable for the problem under consideration and gives rise to an acceptable trade-off between accuracy and computational tractability.

4.2 2313-node distribution system

To validate the scalability of the proposed model for large-sized networks, results for a real Colombian system are presented. This system consists of 2307 load nodes, 2335 branches, and six substations. The nominal voltage of the system is 14.4 kV. Following the increase in the demand, the system's operation became infeasible since the current through some circuits exceeded the maximum limit allowed for the existing conductor, revealing the necessity to plan the installation of distribution system reinforcements. Complete information for the 2313-node distribution system is presented in [29].

DSP simulations are carried out only for the conditions established in Case A-IV considered for the 69-node system, i.e., considering both network reconfiguration and the voltage-dependent load model. For this system, this case is referred to

Table 6: Overview of the Solution for the 2313-Node System

Results		Case B-IV
Investment cost ($\times 10^3$ US$)	Conductors	17.06
	CBs	41.98
	VRs	11.21
	Biomass DG units	285.33
	PV units	169.50
	WT units	4,496.67
	ES units	150.00
Total investment cost ($\times 10^3$ US$)		5,171.75
Total operation cost ($\times 10^3$ US$)		75,292.30
Total cost ($\times 10^3$ US$)		80,464.05
Minimum voltage magnitude (p.u.)		0.95
Maximum voltage magnitude (p.u.)		1.02
Annual CO_2 emissions ($\times 10^3$ tonnes)		80.00

Table 7: Investments Plan for the 2313-Node System

Investment option	Case B-IV
Replacement of conductors (branch ij, type)	392-374, II; 398-494, II; 426-1622, II; 494-389, II; 497-392, II; 499-497, II; 499-1622, II; 501-389, II; 374-501, II; 390-500, II; 500-426, II; 588-558, II; 1309-588, II; 1311-390, II
Network reconfiguration (open branches)	1178-205; 1301-1279; 1302-94; 484-992; 192-961; 505-2297; 650-741; 646-816; 1308-644; 110-122; 175-139; 366-272; 594-619; 646-602; 746-1853; 816-793; 919-853; 939-933; 989-1052; 969-1045; 1261-2297; 1284-1185; 1299-586; 1300-349; 1303-396; 186-71; 655-572; 725-606
VRs (branch ij, type)	6-19, II; 173-174, II; 671-678, II
CBs (node i, number of units)	1035, 4; 2084, 4; 288, 2; 481, 4; 999, 2
Biomass DG units (node i, type)	1080, I; 1372, I; 2199, I; 284, I; 476, I; 794, I; 886, I; 991, I
WT units (node i, number of units)	1584, 22; 414, 1; 470, 12; 614, 7; 958, 8
PV units (node i, number of units)	736, 5; 84,1
ES units (node i, number of units)	1151, 5; 1421, 5; 1759, 5

as Case B-IV. For this study, we consider that the planning strategy is based on an energy policy that limits the CO_2 emissions to 80,000 tonnes during the planning horizon considered. The lower and upper voltage magnitude limits are 0.95 p.u. and 1.05 p.u., respectively. The planning horizon is five years. The demand is estimated based on an annual average growth of 3%. The number of centroids is $k = 2$, thereby obtaining 16 operation scenarios. It is considered an annual interest rate of 10%. The number of blocks used in the piecewise linearization is $\Psi = 10$.

Table 6 shows the planning costs, while Table 7 shows the investment strategy in assets that must be installed in the network. The planning strategy consists of replacing the conductors of 14 branches with conductors of type II; installing three CB units with four 300 kVAr modules at nodes 1035, 2084, and 481, and two CB units with two 300 kVAr modules at nodes 288 and 999; installing three VRs of type II on branches 6-19, 173-174, and 671-678; installing eight biomass DG unit of type I at nodes 1080, 1372, 2199, 284, 476, 794, 886, and 991; installing 22 400 kW WT units at node 1584, one 400 kW WT unit at node 414, twelve 400 kW WT units at node 470, seven 400 kW WT units at node 614, and eight 400 kW WT units at node 958; installing five 100 kW PV units at node 736, and one 100 kW PV units at node 84; installing five 50 kW

ES units at nodes 1151, 1421, and 1759. The computational time to solve Case B-IV for this system is 116.35 h, which is acceptable in a planning context for a large-sized real-world system. Operational results for the 2313-node distribution system are presented in [29].

5. Discussion

In this section, the results obtained for both test systems are analyzed and discussed.

5.1 69-node distribution system

The relevance of including network reconfiguration within the DSP problem can be analyzed by comparing Case A-I and Case A-II. Note that Case A-I represents the way in which the DSP problem considering CO_2 emissions mitigation has usually been approached [8]–[16]. As Table 3 shows, when considering network reconfiguration: (i) the total number of branches whose conductor must be replaced decreases by three branches; (ii) the network topology changes; (iii) the total number of VRs units installed decreases in one unit; and (iv) the total number of PV units installed decreases in one unit. On the other hand, despite the increase in the computational effort in Case A-II, network reconfiguration presents advantages, since it does not involve any investment costs. Table 2 shows that, by considering a variable topology in the DSP problem, it becomes possible to find a solution that is 0.47% cheaper than by considering a fixed topology, given that modifying the network topology causes that the investment in some network assets become unnecessary, reducing the investment cost in 0.91%, and the network operating costs in 0.15%.

The impact of considering the voltage-dependent load model in the DSP problem can be analyzed by comparing Case A-I and Case A-III. As it can be verified in Table 3, there are important changes in the investment plans of these two cases: (i) the total number of CBs installed increases in one unit; (ii) the total number of VRs installed increases in five units; (iii) the total number of PV units installed decreases in six units; (iv) the total number of WT units installed decreases in five units, and (v) the total number of ES units installed decreases in two units. Modeling the demand as voltage-dependent load allows the model to take advantage of the conservation voltage reduction strategy, which consists of reducing grid voltage levels in order to reduce the load. In this way, to exert voltage control on the load, the model prioritizes the installation of equipment such as VRs, which helps to carry out this task. In addition, Table 2 shows that, when considering the voltage-dependent load model, investment costs are 12.53% lower and a 7.82% reduction in total cost is achieved.

The importance of considering both network reconfiguration and the voltage-dependent load model together as part of the DSP problem can be analyzed by comparing Case A-I with Case A-IV. When network reconfiguration is considered and the load is modeled as voltage-dependent, the following changes to the planning strategy occur: (i) the total number of branches whose conductors must be replaced decreases by three branches; (ii) the network topology changes; (iii) the number of VRs installed increases in five units; (iv) the total number of CBs installed decreases in one unit; (v) the number of PV

units installed decreases in eight units; and (vi) the number of WT units installed decreases in four units. As it can be observed in Table 2, the total cost of the planning strategy obtained for Case A-IV is 8.31% cheaper than the total cost obtained for Case A-I, and the investment cost is reduced by 13.59%. The results of Case A-IV show that the energy savings achieved with voltage control and network reconfiguration help to achieve environmental objectives (lower CO_2 emissions) at a lower investment cost.

The 8.31% reduction in the total investment cost verified when the investment plan of Case A-I is compared with the plan of Case A-IV and the reduction of 3.47% in the total costs when the solution considering the optimal operation of the system planned in Case A-I, evaluated using the voltage-dependent load model, is compared with the solution of Case A-IV, evidence the importance of accounting for both a voltage-dependent load model and network reconfiguration in the DSP problem.

5.2 2313-node distribution system

The solution obtained for the 2313-node distribution system in the previous section is assessed with that attained by disregarding investment in new components, i.e., considering only the existing network assets during the whole planning horizon. It is worth mentioning that for the case with no investments the system operation is infeasible, as some circuits exceed the current limits allowed for the existing conductors due to the increase in demand at the end of the planning horizon. Thus, for comparison purposes, in order to obtain a feasible solution for the case with no investments, the current limit constraint (24) was relaxed. Doing so, the operating cost and CO_2 emissions of the network were US$ $84{,}848.63\times10^3$ and 91,352.86 tonnes, respectively.

Table 6 shows that the total cost is 5.17% lower when compared to the network operating cost for the case disregarding investments, thereby revealing the cost-effectiveness of the proposed investment plan over the case where no investment is made. On the other hand, the network's CO_2 emissions for the solution attained by the proposed planning model are 12.43% lower than those obtained with no investment, which reveals the environmental benefits of the proposed investment alternatives. Finally, the suitable computational performance obtained for this large-sized real-world system validates the scalability and computational effectiveness of the proposed approach.

6. Conclusion

In this article, a novel two-stage stochastic programming model is presented to address the medium-term reinforcement planning of active distribution networks taking into account multiple investment alternatives, network reconfiguration, and CO_2 emissions limit. Investment alternatives jointly comprise the replacement of overloaded conductors, the installation of voltage control equipment, such as capacitor banks and voltage regulators, and the installation of distributed energy resources, such as renewable non-dispatchable and dispatchable generators, and energy storage units. The model addresses the

uncertainties of the demand for electricity, energy price at the substation, solar irradiation, and wind speed through a set of representative scenarios. In contrast to conventional planning methods, the proposed approach models the load as voltage-dependent in order to achieve substantial reductions in energy consumption.

The results for the 69-node system show that lower total costs can be achieved by including network reconfiguration in the planning alternatives, as this option does not require any kind of investment, and a reduction in network operating costs can be achieved by modifying its topology. On the other hand, the deployment of renewable distributed generation (DG) units helps to the reduction of CO_2 emissions, which has a positive environmental impact. Although the installation of such technology increases investment costs, this cost is offset by a decrease in operating costs. In addition, the deployment of renewable DG units helps to prevent the distribution company from being penalized for exceeding the CO_2 emissions limits allowed. Results also show that modeling the load as voltage-dependent significantly reduces costs compared to modeling the load as constant power. Such a reduction can be seen, in particular, in the investment costs. For the 2313-node system, the results (i) substantiate the cost effectiveness and environmental benefits of the solution obtained and (ii) demonstrate that the proposed model is scalable and can be applied to medium- and large-sized real systems.

Further work will address the consideration of additional practical modeling aspects such as reliability, demand response, and unbalanced systems. Future research will also be devoted to extending the model for long-term planning by considering the installation of new feeders and new substations. Finally, research efforts will also be conducted to the use of alternative techniques to generate scenarios characterizing uncertainty.

7. Acknowledgment

This work was supported by the Brazilian National Council for Scientific and Technological Development (CNPq), under grants 141985/2017-8 and 310299/2020-9, the Coordination for the Improvement of Higher Education Personnel (CAPES) – Finance Code 001 and grant 88887.371636/2019-00, and the São Paulo Research Foundation (FAPESP), under grants 2015/21972-6, 2018/20355-1, and 2019/19632-3. Also, this work was supported in part by the Ministry of Science, Innovation, and Universities of Spain, under Projects RTI2018-096108-A-I00 and RTI2018-098703-B-I00 (MCIU/AEI/FEDER, UE); and by the Universidad de Castilla-La Mancha, under Grant 2021-GRIN-30952.

References

[1] Georgilakis PS, Hatziargyriou ND. A review of power distribution planning in the modern power systems era: models, methods and future research. Electr Power Syst Res 2015;121:89–100. doi:10.1016/j.epsr.2014.12.010.

[2] Georgilakis PS, Hatziargyriou ND. A review of power distribution planning in the modern power systems era: Models, methods and future research. Electr Power Syst Res 2015;121:89–100. doi:10.1016/j.epsr.2014.12.010.

[3] Li R, Wang W, Chen Z, Jiang J, Zhang W. A review of optimal planning active distribution system: Models, methods, and future researches. Energies 2017;10:1715. doi:10.3390/en10111715.

[4] Vahidinasab V, Tabarzadi M, Arasteh H, Alizadeh MI, Mohammad Beigi M, Sheikhzadeh HR, et al. Overview of electric energy distribution networks expansion planning. IEEE Access 2020;8:34750–69. doi:10.1109/ACCESS.2020.2973455.

[5] Karimi-Arpanahi S, Jooshaki M, Moeini-Aghtaie M, Abbaspour A, Fotuhi-Firuzabad M. Incorporating flexibility requirements into distribution system expansion planning studies based on regulatory policies. Int J Electr Power Energy Syst 2020;118:105769. doi:10.1016/j.ijepes.2019.105769.

[6] Sutherland BR. Tax carbon emissions and credit removal. Joule 2019;3:2071–3. doi:10.1016/j.joule.2019.08.024.

[7] Yi B-W, Xu J-H, Fan Y. Coordination of policy goals between renewable portfolio standards and carbon caps: a quantitative assessment in China. Appl Energy 2019;237:25–35. doi:10.1016/j.apenergy.2018.12.015.

[8] Rocha P, Das TK, Nanduri V, Botterud A. Impact of CO_2 cap-and-trade programs on restructured power markets with generation capacity investments. Int J Electr Power Energy Syst 2015;71:195–208. doi:10.1016/j.ijepes.2015.02.031.

[9] Rodrigues JFD, Wang J, Behrens P, de Boer P. Drivers of CO_2 emissions from electricity generation in the European Union 2000–2015. Renew Sustain Energy Rev 2020;133:110104. doi:10.1016/j.rser.2020.110104.

[10] Ehsan A, Yang Q. State-of-the-art techniques for modelling of uncertainties in active distribution network planning: a review. Appl Energy 2019;239:1509–23. doi:10.1016/j.apenergy.2019.01.211.

[11] Wang S, Luo F, Dong ZY, Ranzi G. Joint planning of active distribution networks considering renewable power uncertainty. Int J Electr Power Energy Syst 2019;110:696–704. doi:10.1016/j.ijepes.2019.03.034.

[12] Shu Z, Jirutitijaroen P. Optimal operation strategy of energy storage system for grid-connected wind power plants. IEEE Trans Sustain Energy 2014;5:190–9. doi:10.1109/TSTE.2013.2278406.

[13] Kayal P, Chanda CK. Strategic approach for reinforcement of intermittent renewable energy sources and capacitor bank for sustainable electric power distribution system. Int J Electr Power Energy Syst 2016;83:335–51. doi:10.1016/j.ijepes.2016.04.029.

[14] Tanaka I, Yuge H, Ohmori H. Formulation and evaluation of long-term allocation problem for renewable distributed generations. IET Renew Power Gener 2017;11:1584–96. doi:10.1049/iet-rpg.2017.0068.

[15] Melgar Dominguez OD, Pourakbari-Kasmaei M, Lavorato M, Mantovani JRS. Optimal siting and sizing of renewable energy sources, storage devices, and reactive support devices to obtain a sustainable electrical distribution systems. Energy Syst 2018;9:529–50. doi:10.1007/s12667-017-0254-8.

[16] Melgar-Dominguez OD, Pourakbari-Kasmaei M, Mantovani JRS. Adaptive robust short-term planning of electrical distribution systems considering siting and sizing of renewable energy based DG units. IEEE Trans Sustain Energy 2019;10:158–69. doi:10.1109/TSTE.2018.2828778.

[17] Home-Ortiz JM, Melgar-Dominguez OD, Pourakbari-Kasmaei M, Mantovani JRS. A stochastic mixed-integer convex programming model for long-term distribution system expansion planning considering greenhouse gas emission mitigation. Int J Electr Power Energy Syst 2019;108:86–95. doi:10.1016/j.ijepes.2018.12.042.

[18] Home-Ortiz JM, Pourakbari-Kasmaei M, Lehtonen M, Sanches Mantovani JR. Optimal location-allocation of storage devices and renewable-based DG in distribution systems. Electr Power Syst Res 2019;172:11–21. doi:10.1016/j.epsr.2019.02.013.

[19] Wu M, Kou L, Hou X, Ji Y, Xu B, Gao H. A bi-level robust planning model for active distribution networks considering uncertainties of renewable energies. Int J Electr Power Energy Syst 2019;105:814–22. doi:10.1016/j.ijepes.2018.09.032.

[20] Melgar-Dominguez OD, Pourakbari-Kasmaei M, Lehtonen M, Mantovani JRS. Voltage-dependent load model-based short-term distribution network planning considering carbon tax surplus. IET Gener Transm Distrib 2019;13:3760–70. doi:10.1049/iet-gtd.2018.6612.

[21] Melgar-Dominguez OD, Pourakbari-Kasmaei M, Lehtonen M, Sanches Mantovani JR. An economic-environmental asset planning in electric distribution networks considering carbon emission trading and demand response. Electr Power Syst Res 2020;181:106202. doi:10.1016/j.epsr.2020.106202.

[22] de Lima TD, Tabares A, Bañol Arias N, Franco JF. Investment & generation costs vs CO_2 emissions in the distribution system expansion planning: A multi-objective stochastic programming approach. Int J Electr Power Energy Syst 2021;131:106925. doi:10.1016/j.ijepes.2021.106925.

[23] Schneider KP, Fuller JC, Tuffner FK, Singh R. Evaluation of conservation voltage reduction (CVR) on a national level. Richland, WA, USA: 2010. doi:10.2172/990131.

[24] Padilha-Feltrin A, Quijano Rodezno DA, Mantovani JRS. Volt-VAr multiobjective optimization to peak-load relief and energy efficiency in distribution networks. IEEE Trans Power Deliv 2015;30:618–26.

doi:10.1109/TPWRD.2014.2336598.

[25] Home-Ortiz JM, Vargas R, Macedo LH, Romero R. Joint reconfiguration of feeders and allocation of capacitor banks in radial distribution systems considering voltage-dependent models. Int J Electr Power Energy Syst 2019;107:298–310. doi:10.1016/j.ijepes.2018.11.035.

[26] Zheng W, Huang W, Hill DJ. A deep learning-based general robust method for network reconfiguration in three-phase unbalanced active distribution networks. Int J Electr Power Energy Syst 2020;120:105982. doi:10.1016/j.ijepes.2020.105982.

[27] Zheng W, Huang W, Hill DJ, Hou Y. An adaptive distributionally robust model for three-phase distribution network reconfiguration. IEEE Trans Smart Grid 2021;12:1224–37. doi:10.1109/TSG.2020.3030299.

[28] Mishra S, Das D, Paul S. A comprehensive review on power distribution network reconfiguration. Energy Syst 2017;8:227–84. doi:10.1007/s12667-016-0195-7.

[29] Mejia MA, Macedo LH, Muñoz-Delgado G, Contreras J, Padilha-Feltrin A. Medium-term planning of active distribution systems considering voltage-dependent loads, network reconfiguration, and CO_2 emissions: test data and results 2021. https://bit.ly/3zg0dFa.

[30] Birge JR, Louveaux F. Introduction to stochastic programming. 2nd ed. New York, NY, USA: Springer New York; 2011. doi:10.1007/978-1-4614-0237-4.

[31] Wu J. Advances in k-means clustering: a data mining thinking. 1st ed. Berlin, Germany: Springer-Verlag; 2012. doi:10.1007/978-3-642-29807-3.

[32] Hajagos LM, Danai B. Laboratory measurements and models of modern loads and their effect on voltage stability studies. IEEE Trans Power Syst 1998;13:584–92. doi:10.1109/59.667386.

[33] Lavorato M, Franco JF, Rider MJ, Romero R. Imposing radiality constraints in distribution system optimization problems. IEEE Trans Power Syst 2012;27:172–80. doi:10.1109/TPWRS.2011.2161349.

[34] Fourer R, Gay DM, Kernighan BW. AMPL: A modeling language for mathematical programming. 2nd ed. Duxbury, MA, USA: Thomson; 2003.

[35] IBM. IBM ILOG CPLEX Optimization Studio 20.1.0 documentation. 2021 n.d. https://www.ibm.com/support/knowledgecenter/SSSA5P_20.1.0/COS_KC_home.html (accessed February 1, 2021).

[36] Baran ME, Wu FF. Optimal capacitor placement on radial distribution systems. IEEE Trans Power Deliv 1989;4:725–34. doi:10.1109/61.19265.